Acta Crystallographica Section F
Structural Biology and Crystallization Communications
ISSN 1744-3091

Crystallization, preliminary crystallographic analysis and phasing of the thiosulfate-binding protein SoxY from *Chlorobium limicola* f. *thiosulfatophilum*

Jan Stout,[a] Lina De Smet,[a] Santosh Panjikar,[b] Manfred S. Weiss,[b] Savvas N. Savvides[a]* and Jozef Van Beeumen[a]*

[a]Department of Biochemistry, Physiology and Microbiology, Laboratory for Protein Biochemistry and Protein Engineering, K. L. Ledeganckstraat 35, Ghent University, 9000 Ghent, Belgium, and [b]EMBL Hamburg Outstation, c/o DESY, Notkestrasse 85, D-22063 Hamburg, Germany

Correspondence e-mail: savvas.savvides@ugent.be, jozef.vanbeeumen@ugent.be

Received 28 July 2006
Accepted 8 September 2006

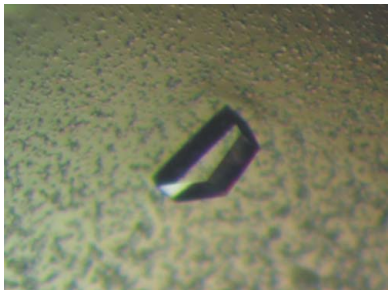

The 22 kDa SoxYZ protein complex from the green sulfur bacterium *Chlorobium limicola* f. *thiosulfatophilum* is a central player in the sulfur-oxidizing (Sox) enzyme system of the organism by activating thiosulfate for oxidation by SoxXA and SoxB. It has been proposed that SoxYZ exists as a heterodimer or heterotetramer, but the properties and role of the individual components of the complex thus far remain unknown. Here, the heterologous expression, purification, and the crystallization of stable tetrameric SoxY are reported. Crystals of SoxY diffract to 2.15 Å resolution and belong to space group $C222_1$, with unit-cell parameters $a = 41.22$, $b = 120.11$, $c = 95.30$ Å. MIRAS data from Pt^{2+}- and Hg^{2+}-derivatized SoxY crystals resulted in an interpretable electron-density map at 3 Å resolution after density modification.

1. Introduction

The SoxY protein is an essential component of the SoxYZ complex, which plays a key role in the sulfur-oxidizing (Sox) multi-enzyme system by virtue of a reactive cysteine residue (Rother *et al.*, 2001). This periplasmic Sox system represents a common platform for the oxidation of sulfide, elemental sulfur and thiosulfate to sulfate in several lithotrophic green sulfur (Verté *et al.*, 2002; Eisen *et al.*, 2002), phototrophic and neutrophilic non-phototrophic proteobacteria (Friedrich, 1998; Friedrich *et al.*, 2001, 2005; Mukhopadhyaya *et al.*, 2000), thereby generating electrons for the respiratory or autotrophic growth of the host.

Although most of the Sox components, SoxYZ, SoxAX, SoxB and SoxCD, have been identified, the structural and molecular basis for their individual mode of action and their role in the formation of productive Sox (sub)complexes remain largely uncharacterized (Rother *et al.*, 2001; Friedrich *et al.*, 2000). Thus far, only structures of the SoxAX complex have been published (Bamford *et al.*, 2002; Dambé *et al.*, 2005).

Binding studies of SoxYZ from *Paracoccus pantotrophus* with several reduced sulfur compounds have demonstrated that SoxYZ can function as the sulfur substrate-binding protein. For this purpose, SoxY uses a conserved C-terminal cysteine that binds the substrate *via* a thioether or thioester bond (Quentmeier & Friedrich, 2001). The coupling of sulfur substrates to SoxY has been proposed to be mediated by the SoxAX complex (Bamford *et al.*, 2002; Friedrich *et al.*, 2001). This newly formed SoxY–sulfur compound adduct would then serve as a substrate for SoxB and SoxCD, which in turn would oxidize the bound sulfur substrate, generating sulfate and free SoxY as end products (Friedrich *et al.*, 2001). Incomplete Sox systems without SoxCD have also been found in *Chlorobiaceae* (Verté *et al.*, 2002; Eisen *et al.*, 2002) and in *Allochromatium vinosum* (Friedrich *et al.*, 2005) and it is also unclear how the oxidation of thiosulfate occurs in these bacteria. It has also been suggested that a disulfide bridge activates the cysteines for binding of reduced sulfur compounds by means of a thiol/disulfide-exchange reaction (Quentmeier *et al.*, 2003). This hypothesis is based on the observation that the C-terminal cysteine is redox-active, having the ability to form a disulfide bridge with another C-terminal cysteine (Quentmeier *et al.*, 2003).

In addition to its sulfur-binding properties, SoxYZ exhibits a dynamic oligomerization behaviour, being able to form heterodimers and heterotetramers. Furthermore, SoxZ of *Thermus thermophilus* has recently been shown to be a stable homodimer on its own (PDB code 1v8h; unpublished work), which indicates that SoxYZ is not an obligate structural complex. Taken together, these observations raise intriguing questions about the versatility of the SoxY and SoxZ molecular scaffolds towards complex formation. Here, we report the successful heterologous expression, purification, crystallization and phasing of a stable tetrameric SoxY protein from *Chlorobium limicola* f. *thiosulfatophilum* as part of a program we have initiated to dissect the SoxYZ complex from this bacterium. With the determination of the SoxY structure, we aim to gain a better understanding of the underlying principles governing its sulfur-binding affinity and its versatile oligomerization behaviour.

2. Materials and methods

2.1. Cloning, overexpression and purification of SoxY

The protein-coding sequence of SoxY without its Tat signal sequence was cloned into the pET20b expression plasmid (Novagen) as a fusion with a *pelB* signal sequence for translocation into the periplasm. An *Nco*I restriction site was introduced for in-frame cloning between the *pelB* signal sequence and the coding sequence of the mature SoxY. From DNA sequencing of the *soxY* gene on the expression plasmid, it was apparent that a conservative point mutation had occurred from glutamate to aspartate at position 14 of the mature SoxY sequence. When transformed into *Escherichia coli* C43(DE3), the construct resulted in substantial amounts of soluble recombinant protein. A 10 ml volume of an overnight preculture at 310 K was inoculated into 1 l Luria–Bertani medium (Sambrook *et al.*, 1989) at 288 K. When the cultures reached an optical density (at 600 nm) of 0.6, isopropyl β-D-thiogalactosidase (IPTG) was added to a final concentration of 0.1 m*M* and the cultures were incubated overnight at the same temperature. After centrifugation, periplasmic extracts of the cell pellets were obtained *via* a cold-shock procedure (De Sutter *et al.*, 1994). The cell pellets were suspended in ice-cold SET buffer [200 m*M* Tris–HCl pH 8.0, 20%(*w*/*v*) sucrose, 1 m*M* EDTA] and incubated on ice for 10 min. After centrifugation and removal of the SET buffer, the cell pellets were resuspended in 5 m*M* ice-cold $MgCl_2$ and were left to stand on ice for 10 min. The resulting cell-free supernatant after centrifugation was diluted twofold in 20 m*M* Tris–HCl pH 8.0 (buffer I) and loaded onto a Q-Sepharose column (Amersham). The flowthrough and one column volume of washing buffer (buffer I) containing SoxY were pooled and used for further separation on a phenyl-Sepharose column. The column (8 ml), loaded with the protein sample, was subjected to a ten column volume linear gradient from 1 *M* $(NH_4)_2SO_4$, 20 m*M* Tris–HCl pH 8.0 to 20 m*M* Tris–HCl pH 8.0. All SoxY-containing fractions were pooled and SoxY was further purified to homogeneity on a Superdex-200 size-exclusion column (Amersham) as a final polishing step. The concentrated protein solution (approximately 8 mg ml^{-1}) was stored at 277 K in 50 m*M* Tris–HCl pH 8.0, 100 m*M* NaCl. The presence of NaCl in the storage solution keeps the recombinant SoxY in a soluble state.

2.2. Crystallization and data collection

All crystallization trials and crystal-growth optimization experiments were performed at 295 K using the hanging-drop vapour-diffusion method. 1 µl drops were prepared by mixing equal volumes of protein solution and precipitant solution and were equilibrated against 1 ml reservoir solution. Structure Screens I and II (Molecular Dimensions Ltd), JB Classic Screens 1–10 (Jena Bioscience) and the PEG/Ion Screen (Hampton Research) were used for initial screening. Promising crystallization leads were optimized *via* testing precipitants having similar physicochemical properties to those of the precipitant in the lead condition, by varying the precipitant concentration and pH, and with the help of additive screens from Molecular Dimensions Ltd.

Native SoxY crystals were mounted in capillaries and their diffraction quality was assessed at room temperature using an in-house Bruker–Nonius FR-591 rotating-anode X-ray generator operating at 45 kV and 90 mA and producing Cu $K\alpha$ X-rays focused with Osmic mirrors to a wavelength of 1.54 Å. The best crystal diffracted to 2.4 Å resolution and was used to collect 110 rotation images with a 1° oscillation angle using a DIP2030b image plate with a crystal-to-detector distance of 175 mm.

For data collection under cryogenic conditions (100 K), native SoxY crystals were transferred to a solution containing 20%(*v*/*v*) PEG 400 in mother liquor and were subsequently flash-cooled by plunging them directly into liquid nitrogen. X-ray diffraction data were collected from single crystals at a wavelength of 1.06 Å at beamline BW7A, DESY, EMBL Hamburg Outstation, Germany. All diffraction data were collected in dose mode using a MAR CCD (MAR Research) detector system. A low-resolution pass followed by a high-resolution pass were recorded from the same crystal at 100 K. For the low-resolution pass, 180 rotation images (8 s per image) were collected with an oscillation angle of 1.0° and a crystal-to-detector distance of 200 mm. For the high-resolution pass, the crystal-to-detector distance was adjusted to 140 mm and 180 rotation images (18 s per image) were again collected with the same oscillation angle. All diffraction data were processed and scaled with the programs *DENZO* and *SCALEPACK* (Otwinowski & Minor, 1997).

Data collection for the screening of heavy-atom derivatives of SoxY crystals was carried out at room temperature and at 100 K. Derivatized crystals were obtained by incubating native SoxY crystals in stabilization buffer (1.6 *M* $NH_4H_2PO_4$, 100 m*M* sodium acetate pH 4.0) containing the target heavy-atom compound at concentrations up to 10 m*M* for a period of 10 min to 16 h (Sun *et al.*, 2002). A back-soaking step was then carried out in stabilization buffer containing no heavy-atom compound. Diffraction data were collected in-house and at beamline BW7A, DESY, EMBL Hamburg Outstation, Germany. Heavy-atom substructures were determined using search procedures implemented in the programs *Auto-Rickshaw* (Panjikar *et al.*, 2005) and *SOLVE* v.2.08 (Terwilliger & Berendzen, 1999). Initial phases were obtained using SAD/MAD and SIR/MIR(AS) approaches implemented in *Auto-Rickshaw* and *SOLVE* v.2.08 and were subsequently improved by electron-density modification procedures implemented in *RESOLVE* v.2.08.

3. Results and discussion

Recombinant SoxY was purified to >95% homogeneity with a yield of 0.3 mg protein per litre of expression culture. Gel-filtration experiments showed that SoxY eluted as a tetramer.

During the initial screening of crystallization conditions, SoxY mainly separated out from the aqueous phase into an oil-like solution. Two conditions were identified as a starting point for further optimization: condition No. 43 [0.2 *M* $NH_4H_2PO_4$, 20%(*w*/*v*) PEG 3350] from the PEG/Ion Screen (Hampton Research), which produced spherulites, and condition No. 39 [0.2 *M* $(NH_4)_2SO_4$, 0.1 *M* sodium acetate pH 4.6, 30%(*w*/*v*) PEG MME 2000] from Structure

Table 1
Statistics of data collection and phasing.

(*a*) Data collection. Values in parentheses refer to the highest resolution shell.

	Native 1	Native 2	K_2PtCl_4	$Hg(OAc)_2$
Temperature (K)	293	100	100	100
X-ray source	FR-591	BW7A	BW7A	BW7A
Wavelength (Å)	1.54	1.06	1.04	1.04
Space group	$C222_1$	$C222_1$	$C222_1$	$C222_1$
Unit-cell parameters (Å)				
a	41.22	40.73	41.92	41.96
b	122.65	120.11	123.25	124.54
c	97.29	95.30	97.29	98.30
Mosaicity (°)	0.28	0.80	0.46	0.87
Resolution range (Å)	20.0–2.39 (2.43–2.39)	99.0–2.15 (2.20–2.15)	30.0–2.8 (2.88–2.80)	30.0–3.1 (3.19–3.10)
No. of observed reflections	48472	102451	46896	22883
No. of unique reflections	10173 (498)	13122 (831)	6533 (509)	4617 (378)
Completeness (%)	100.0 (100.0)	98.1 (97.8)	99.9 (100.0)	92.1 (91.1)
Average $I/\sigma(I)$	17.5 (3.4)	33.4 (5.6)	22.2 (14.5)	16.9 (11.3)
R_{merge}† (%)	8.4 (53.2)	5.5 (39.3)	7.3 (13.9)	7.3 (12.8)

(*b*) MIRAS phasing statistics for Pt^{2+}- and Hg^{2+}-derivatives.

	K_2PtCl_4	$Hg(OAc)_2$	
Resolution range (Å)	25.0–3.0		
Figure of merit	0.49		
Phasing power centrics/acentrics	0.92/1.04	0.66/0.71	
R_{iso}‡ (%)	19.3	11.6	
No. of sites	1	2	
Occupancy	0.61	0.24	0.12
x (Å)	12.284	18.674	2.056
y (Å)	21.199	0.623	26.402
z (Å)	1.070	7.297	4.522
B_{iso}	60.0	60.0	47.7

† $R_{merge} = \sum_h \sum_i |I(h,i) - \langle I(h)\rangle| / \sum_h \sum_i I(h,i)$, where $I(h,i)$ is the intensity of the *i*th measurement of reflection *h* and $\langle I(h)\rangle$ is the average value over multiple measurements. ‡ $R_{iso} = \sum_h \big||F_{PH}(h)| - |F_P(H)|\big| / \sum_h |F_P(h)|$, where $|F_{PH}(h)|$ and $|F_P(h)|$ are the amplitudes of the derivative and native structure factors with index *h*, respectively.

Screen II (Molecular Dimensions Ltd), which yielded small crystals. Several sulfate-, phosphate- and ammonium-containing salts were tested in combination with PEG MME 2000 at various pH values (4–8) to optimize crystal growth. Crystal growth was pH-dependent (pH 3.8–4.5) and large irregularly formed crystals appeared in 1.4 *M* $NH_4H_2PO_4$, 100 m*M* sodium acetate pH 4.0. This condition was therefore chosen for further optimization using an additive screen (Additive Screen I, Molecular Dimensions Ltd). The use of 5 m*M* dithiotreitol (DTT) as an additive drastically improved the quality of the SoxY crystals. Large rectangular plates measuring 0.04 × 0.1 × 0.3 mm (Fig. 1) were grown at room temperature by equilibrating 4 µl drops, set up by mixing 2 µl 8 mg ml^{-1} SoxY solution with 1.6 µl precipitant solution (1.4 *M* $NH_4H_2PO_4$, 100 m*M* sodium acetate pH 4.0) and 0.4 µl 50 m*M* DTT, against 1 ml precipitant solution in the reservoir. Crystals appeared after 3 d and reached their maximum size after one week.

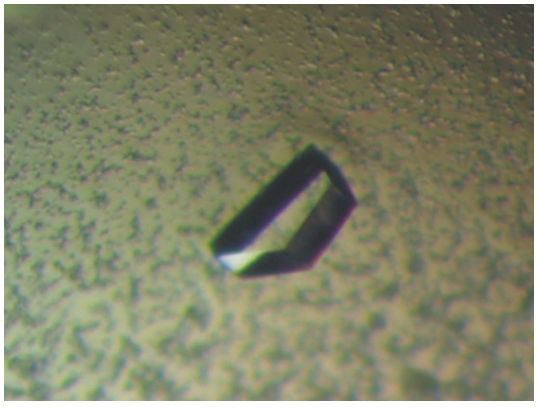

Figure 1
SoxY crystal grown in 1.4 *M* $NH_4H_2PO_4$, 100 m*M* sodium acetate pH 4.0, 5 m*M* DTT. The longest dimension is ∼0.3 mm.

Complete data sets for native SoxY were collected from a single crystal at 100 K and room temperature to 2.15 and 2.4 Å resolution, respectively (Table 1). On the basis of a calculated molecular weight of 13 042 Da for a SoxY monomer and the size of the *C*-centred orthorhombic unit cell, the asymmetric unit was estimated to contain two SoxY subunits. This suggested that a tetramer of SoxY is generated by a crystallographic twofold axis from a dimer in the asymmetric unit. The solvent content of the crystal was 42.8%, with a volume-to-weight ratio of 2.23 Å^3 Da^{-1}. These values are within the frequently observed ranges for protein crystals (Matthews, 1968).

Owing to the ease of reproducibly growing large numbers of high-quality SoxY crystals, we decided to screen a wide range of heavy-atom compounds to assess their usefulness for experimental phasing. Firstly, room-temperature X-ray diffraction data from several heavy-atom-derivative SoxY crystals were collected and analyzed with *SOLVE* v.2.08 (Terwilliger & Berendzen, 1999) to locate potential heavy-atom sites. K_2PtCl_4-derivatized crystals gave promising results. This derivative was subsequently reproduced and used for a MAD phasing experiment at 100 K using synchrotron radiation. The resulting phases, however, were of insufficient quality to produce an interpretable electron-density map, most likely owing to the low occupancy of the heavy atoms. As a potential remedy, the quick-soaking method described by Sun *et al.* (2002) was employed as a heavy-atom-derivatization procedure. Data collection on K_2PtCl_4- and $Hg(Ac)_2$-derivatized crystals was carried out using synchrotron radiation at EMBL beamline BW7A at 100 K. These derivative data sets were evaluated at the EMBL beamline using the SIRAS protocol in *Auto-Rickshaw*, the EMBL-Hamburg automated crystal structure-determination platform (Panjikar *et al.*, 2005). In each case, the input diffraction data were prepared and converted for use in *Auto-Rickshaw* using programs from the *CCP*4 suite (Collaborative Computational Project, Number 4, 1994). F_A values were calculated using the program *SHELXC* (Sheldrick *et al.*, 2001) and substructure atoms were found using the program *SHELXD* (Schneider & Sheldrick, 2002). The correct hand for the substructure was determined using

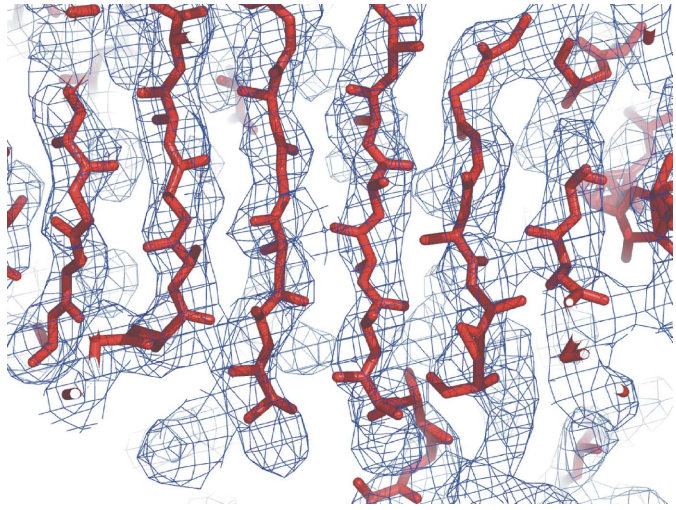

Figure 2
Figure of merit MIRAS electron-density map after density modification, contoured at 1.0σ, $\rho_{r.m.s.d.}$. The partially traced main chain is shown in red.

the programs *ABS* (Hao, 2004) and *SHELXE* (Sheldrick, 2002). The occupancy of all substructure atoms was refined using the program *BP*3 (Pannu *et al.*, 2003). The initial phases were improved by density modification and phase extension to 3.0 Å resolution using the program *DM* (Cowtan, 1994) and the map was found to be interpretable. The derivatized crystals demonstrated the presence of one high-occupancy Pt^{2+} site and two low-occupancy Hg^{2+} sites, respectively. Phase calculation and refinement of both derivatives using the MIRAS protocol in *SOLVE* v.2.08 led to an improved experimental electron-density map at 3.0 Å resolution with a clear protein–solvent boundary and several crude secondary-structure features. The MIRAS experimental phases were drastically improved by iterative rounds of maximum-likelihood electron-density modification in *RESOLVE* v.2.08 (Terwilliger, 2000). The resulting electron-density map allowed modelling of about 70% of the main-chain atoms for both monomers (Fig. 2), which at first sight are related by a non-crystallographic twofold axis. However, implementation of this initial NCS relationship in the density-modification procedure did not lead to a further improvement of the electron density. Model building and refinement of the structure are under way.

We gratefully acknowledge access to the EMBL beamline BW7A at the DORIS storage ring, DESY, Hamburg. JS is a research fellow of the 'Instituut voor de aanmoediging van Innovatie door Wetenschap en Technologie en Vooruitgang in Vlaanderen' (IWT). JVB is indebted to the 'Fonds voor Wetenschappelijk Onderzoek-Vlaanderen' (FWO-Flanders; grant G.0330.03).

References

Bamford, V. A., Bruno, S., Rasmussen, T., Appia-Ayme, C., Cheesman, M. R., Berks, B. C. & Hemmings, A. M. (2002). *EMBO J.* **21**, 5599–5610.
Collaborative Computational Project, Number 4 (1994). *Acta Cryst.* D**50**, 760–763.
Cowtan, K. (1994). *Jnt CCP4/ESF–EACBM Newsl. Protein Crystallogr.* **31**, 34–38.
Dambé, T., Quentmeier, A., Rother, D., Friedrich, C. & Scheidig, A. J. (2005). *J. Struct. Biol.* **152**, 229–234.
De Sutter, K., Hostens, K., Vandekerckhove, J. & Fiers, W. (1994). *Gene*, **141**, 163–170.
Eisen, J. A. *et al.* (2002). *Proc. Natl Acad. Sci. USA*, **99**, 9509–9514.
Friedrich, C. G. (1998). *Adv. Microb. Physiol.* **39**, 235–289.
Friedrich, C. G., Bardischewsky, F., Rother, D., Quentmeier, A. & Fischer, J. (2005). *Curr. Opin. Microbiol.* **8**, 253–259.
Friedrich, C. G., Quentmeier, A., Bardischewsky, F., Rother, D., Kraft, R., Kostka, S. & Prinz, H. (2000). *J. Bacteriol.* **182**, 4677–4687.
Friedrich, C. G., Rother, D., Bardischewsky, F., Quentmeier, A. & Fischer, J. (2001). *Appl. Environ. Microbiol.* **67**, 2873–2882.
Hao, Q. (2004). *J. Appl. Cryst.* **37**, 498–499.
Matthews, B. W. (1968). *J. Mol. Biol.* **33**, 491–497.
Mukhopadhyaya, P. N., Deb, C., Lahiri, C. & Roy, P. (2000). *J. Bacteriol.* **182**, 4278–4287.
Otwinowski, Z. & Minor, W. (1997). *Methods Enzymol.* **276**, 307–326.
Panjikar, S., Parthasarathy, V., Lamzin, V. S., Weiss, M. S. & Tucker, P. A. (2005). *Acta Cryst.* D**61**, 449–457.
Pannu, N. S., McCoy, A. J. & Read, R. J. (2003). *Acta Cryst.* D**59**, 1801–1808.
Quentmeier, A. & Friedrich, C. G. (2001). *FEBS Lett.* **503**, 168–172.
Quentmeier, A., Hellwig, P., Bardischewsky, F., Grelle, G., Kraft, R. & Friedrich, C. G. (2003). *Biochem. Biophys. Res. Commun.* **312**, 1011–1018.
Rother, D., Henrich, H. J., Quentmeier, A., Bardischewsky, F. & Friedrich, C. G. (2001). *J. Bacteriol.* **183**, 4499–4508.
Sambrook, J., Fritsch, E. F. & Maniatis, T. (1989). *Molecular Cloning. A Laboratory Manual*, 2nd ed. New York: Cold Spring Harbor Laboratory Press.
Schneider, T. R. & Sheldrick, G. M. (2002). *Acta Cryst.* D**58**, 1772–1779.
Sheldrick, G. M. (2002). *Z. Kristallogr.* **217**, 644–650.
Sheldrick, G. M., Hauptman, H. A., Weeks, C. M., Miller, R. & Usón, I. (2001). *International Tables for Crystallography*, Vol. *F*, edited by M. G. Rossmann & E. Arnold, pp. 333–345. Dordrecht: Kluwer Academic Publishers.
Sun, P. D., Radaev, S. & Kattah, M. (2002). *Acta Cryst.* D**58**, 1092–1098.
Terwilliger, T. C. (2000). *Acta Cryst.* D**56**, 965–972.
Terwilliger, T. C. & Berendzen, J. (1999). *Acta Cryst.* D**55**, 849–861.
Verté, F., Kostanjevecki, V., De, S. L., Meyer, T. E., Cusanovich, M. A. & Van Beeumen, J. J. (2002). *Biochemistry*, **41**, 2932–2945.